Academic Journal of Science and Technology,
October, 2024, vol.4, No.1, p214-221

Synthesis and Characterization of Iron, Titanium and their Mixture with Benzene-1,3,5-Tricarboxylic Acid Framework

Abdussallam N. Eldewik[1], Safa. A. Flaifel [1*].

1. Department of Chemistry, The Libyan Academy for Postgraduate Studies

ABSTRACT

Metal-organic frameworks (MOFs, also known as coordination polymers), are a new class of crystalline porous materials that consist of metal centers and/or metal clusters connected by organic linkers.

This project is concerned with the synthesizing and characterization of mixed-metal metal-organic frameworks (MM-MOFs) of 1,3,5-Tri-Carboxylic Acid Benzene (BTC), M-Fe-BTC, where M = Ti+3, by using the Solvothermal method .The MM-MOFs' powder X-ray diffraction patterns were similar to those of MIL (100). The results of scanning electron microscopy show that most of them are nanomaterials. The six samples had varying amounts of iron and titanium, according to the EDX results. The FT-IR results support the XRD outcomes .Thermal analysis demonstrates multiple stages of decomposition, and the materials show thermal stability up to 450 °C. UV-Vis Diffuse Reflectance confirmed that all samples, with the exception of sample No. 1 (insulator), are semiconductors.

KEYWORDS: *MOFS, Mixed-metal metal−organic frameworks (MM-MOFs).*

** Corresponding author:* safaflaifel7@gmail.com

INTRODUCTION

Metal-organic frameworks (MOFs, also known as coordination polymers) [1], are a new class of crystalline porous materials [2] consisting of metal centers and/or metal clusters connected by organic linkers [3]. The organic units are typically mono-, di-, tri-, or tetravalent ligands [4], forming 3-D porous structures with 1-D, 2-D, or 3-D channel systems [3]. The structure and characteristics of the MOF are significantly impacted by the choice of metal and linker. For example, the metal's coordination preference influences the size and shape of pores by dictating how many ligands can bind to the metal and in which direction [5].

MOFs consist of inorganic and organic units. The (linkers/bridging ligands) are the organic units, carboxylates, or anions, such as phosphonate, sulfonate, and heterocyclic compounds are the most common example of them [6]. For the construction of metal-organic frameworks, Poly carboxylic acids are among the most attractive building blocks due to their versatile coordination modes, which prompted several studies to ascertain routes to predictable metal-carboxylate motifs and to design new open framework structures. Some research relates to the use of dicarboxylate, tricarboxylate, and tetra carboxylate ligands, which are inter-bridged by mono- or multi-nuclear metal nodes, leading to stable MOFs with permanent porosity. Benzene-1,3,5-tricarboxylic acid (H3BTC, tri mesic acid) has been extensively used in its various degrees of deprotonation as a bridging ligand in the synthesis of multidimensional MOFs [7].

Iron is an attractive transition element because it is readily available, inexpensive, environmentally friendly, nontoxic, and exhibits interesting redox behavior. Fe-BTC is an iron (III) carboxylate MOF that has initially been developed by the collaboration between the CNRS-Institute for Lavoisier (ILV; Prof. G. Ferrey and Dr. C. Serre) and the Korea Research Institute of Chemical Technology (KRICT; Dr. J.-S. Chang and Dr. Y.K. Hwang). In fact, it is one of the most porous MOFs that can be prepared by large-scale hydrothermal synthesis [8]. Titanium (Ti)-based metal-organic frameworks (MOFs) have attracted considerable attention due to their low toxicity, abundance in the earth's crust, and unique photocatalytic properties of the Ti element. The Ti-BTC described by Marti-Gastaldo et al. is based on the combination of BTC ligand and Ti3(μ3-O) trimer [9]. The aim of this study is to synthesize and characterize Fe-BTC and Ti-BTC using optimal chemical methods and to determine the crystal structures of Fe-BTC, Ti-BTC, and their mixtures.

MATERIALS AND METHODS

MOFs were frequently synthesized using the conventional Solvothermal method by heating a mixture of metal salt and organic linker in a solvent that typically contains formamide to temperatures near or above the boiling point of the solvent. This method is widely used since it is commonly used to synthesize other porous materials and often yields crystals suitable for XRD [10].

MATERIALS

Solvents and materials used for preparation were: DMF (99.9%) (ROMIL-SPS), deionized water, iron chloride (III) $FeCl_3$ (aq) by **Riedel-**de Haën AG (0.166M), 1,3,5-benzenetricarboxylic acid (H3BTC, 99%) was supplied by Aldrich, and titanium chloride (0.166M) (III) $TiCl_3$ by Alfa Aesar Chemicals. All the chemicals were used without further purification, and the reaction solutions were prepared in a volumetric flask.

SYNTHETIC PROTOCOLS

FeBTC and TiBTC were synthesized following a previously reported study [11]. Briefly, 60 ml of $FeCl_3$, $TiCl_3$ solutions (0.166 M) was added gradually to 60 ml of BTC solution (1:1 ratio). The homogeneous solution was mixed in a 120 mL Teflon and stirred for ~1 hour using a magnetic stirrer plate. After stirring, the sample was put in a sealed autoclave and placed in a preheated oven at 120 °C for overnight. PH and temperature for the mixture were measured (0.5, 120) before placing the sample in the oven, as shown in Table1. After that, the sample was cooling to room temperature for approximately 24h.The resulted product was collected by filtration and rinsed with about 10ml fresh DMF, and the solid was allowed to dry in the drier at

35-38°C for ~24h., finally the product was weighed. And all the important information related to the samples is collected in Table1.

Sample No	proportion	Synthetic protocol	pH	Temp/C^0	Product/g
Sample 1	100% Fe	Solvo-thermal	0.5	120	1.5
Sample 2	90%Fe,10%Ti	Solvo-thermal	0.5	120	1.238
Sample 3	70%Fe,30%Ti	Solvo-thermal	0.5	120	0.5
Sample 4	50%Fe,50%Ti	Solvo-thermal	0.7	120	0.5
Sample 5	20%Fe,80%Ti	Solvo-thermal	0.6	120	1.25
Sample 6	100%Ti	Solvo-thermal	1.3	120	0.26

Table 1: Samples parameter preparation and their PH, temperature, and weight product (1-6)

CHARACTERIZATION

The characterization of the MOFs products were investigated using scanning electron microscopy (SEM), Fourier transform infrared spectroscopy (FTIR), thermal gravimetric analysis (TGA), X-ray diffraction (XRD), energy dispersive X-ray (EDX), and UV-VIS diffuse reflectance.

RESULTS AND DISCUSSION:

X-RAY DIFFRACTION (XRD)

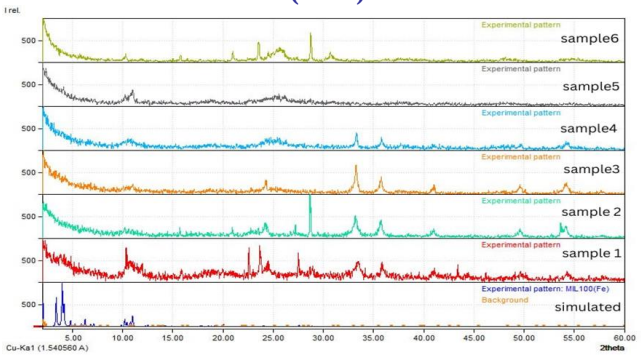

Figure 1: Powder XRD spectra for the sample (1-6) and the simulated pattern of MIL100(Fe).

From figure 1 and comparing the results of the previous samples with the resulted XRD spectrum of the MIL-100, it was found that the samples follow the MIL-100 (simulated) pattern. The PXRD patterns of MM-MOFs display that the modified MOFs are isostructural to Fe-BTC.

MIL-100 (Fe) is an iron (III) carboxylate that was first created through cooperation between the Korea Research Institute of Chemical Technology (KRICT; Dr. J.-S. Chang and Dr. Y.K. Hwang) and the CNRS-Institute for Lavoisier (ILV; Prof. G. Férey and Dr. C. Serre).

The diffractogram of the synthesized materials, as seen in Figure 1, generally agrees with the simulated powder pattern from the single crystal data of MIL-100 (Fe), with the main 2θ on 7.11, 10.9, 10.03, 20.15, and 25. This proves beyond any doubt that MIL-100 (Fe) was synthesized. The diffraction pattern looks broad and shows that the semi-crystalline nature of the material crystal has a specific phase; its size (crystallite size) can be ascertained using X-ray diffraction [12]. Equation which formulates Debye Scherrer's equation, is used to determine the primary peaks of the pattern diffractogram.

D = K. λ/βcos θ [13], where D is the size of the crystallite, K is the Scherrer constant (0.9), λ is the X-ray wavelength (0.15406 nm), β is the Full Width at Half Maximum (FWM, radians), and θ is the peak position.

The lattice parameters can be calculated using the following equation:

sin2 θ = (h2+k2+l2) (λ2 /4a2)

from the previous equations we can determine the size and shape of the Crystal as shown in Table 2:

Table 2: Crystall Size and shape of samples (1-6)

Sample No	Size (nm)	Crystal type
1	1.58	Face-centered cubic
2	1.19	Face-centered cubic
3	1.2	Diamond Cubic
4	1.6	Face-centered cubic
5	1.0	Face-centered cubic
6	1.19	Diamond Cubic

EDX AND SEM RESULTS

From the EDX results, the amount of Iron and Titanium have been calculated within each sample, as shown in Table 3.

Table3: Iron and Titanium amount of the Samples (1-6)

Sample No	Fe	Ti
1	1	0
2	0.7	0.3
3	0.5	0.5
4	0.02	0.98
5	0.3	0.7
6	0	1

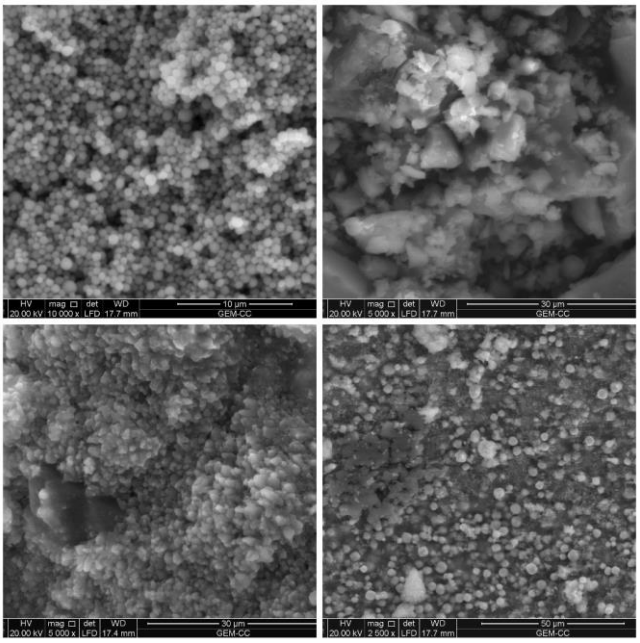

Figure2: SEM Results for the samples (1-6)

From the SEM Results, the material samples appear to be nanoparticle-sized based on the figure2, which is in agreement with the information gained from the XRD results (Debye Scherrer's equation).

Figure 3 shows FT-IR spectra of BTC ligand and resulted samples. It is evident that every sample has the same ligand pattern. The notable in stretching vibration from the C=O acid ligand from 1697 cm-1 (free ligand) to 1607 cm-1 prove that BTC's C=O carboxyl group has been deprotonated and intercalated with M3+ to create MIL-100.

The two sharp bands at 1250 and 1200 cm−1 are attributed to asymmetric (νas (CO)) and symmetric (νs (CO)) vibrations of carboxyl groups, respectively. This result confirms the presence of the tricarboxylate ligands [20]. In addition, from the vibration at 410–420 cm-1 it is possible to identify the features of Fe-O stretching vibrations in which the oxygen atom coordinates with Fe3+. The broad peak at 2514–3360 cm-1, corresponds to the OH stretching absorption of the carboxyl group and shifted from 3094–3624 cm-1 which indicates the presence of water molecules bonding the M-M trimeic unit on MIL-100. (Because of the interactions between the water molecules, this peak is typically broad. This wide peak demonstrates the hydrophilicity of the samples [14], and the aromatic benzene ring observe in bands below 1300,[15].

FT-IR RESULTS

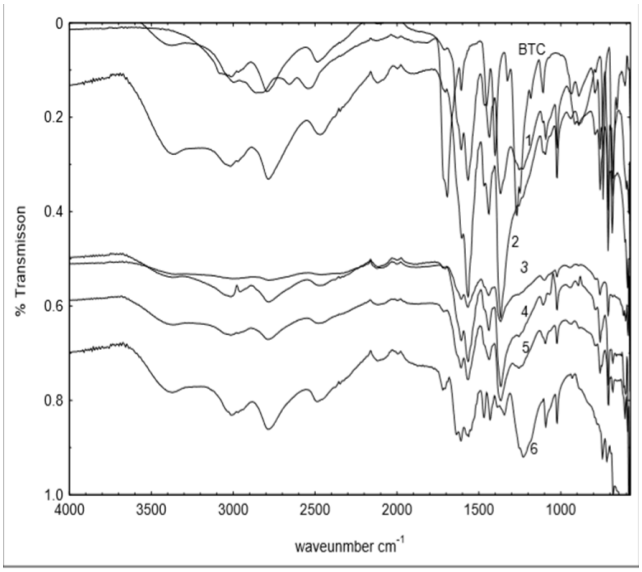

Figure3. FT-IR spectra of the ligand BTC and samples (1-6).

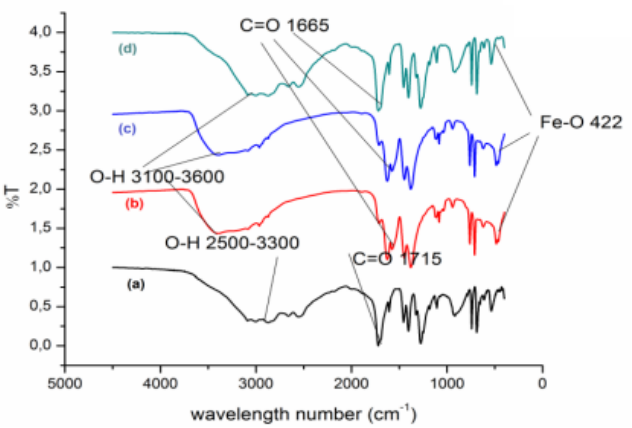

Figure 4: FT-IR spectra of (a) ligand: 1,3,5-benzene tricarboxylic acid and MIL-100(Fe) which electrochemically synthesized (after and before activation, b and c) and hydrothermal (d) [15].

Additionally, the bands that show up at around 744, 1026, 1360, and 1610 cm^{-1} are bands that show the compound contains Iron; according to [16] the O-H stretching peak is located at 3400 cm^{-1}. According to [17], this band additionally demonstrates titanium's presence in the compoun

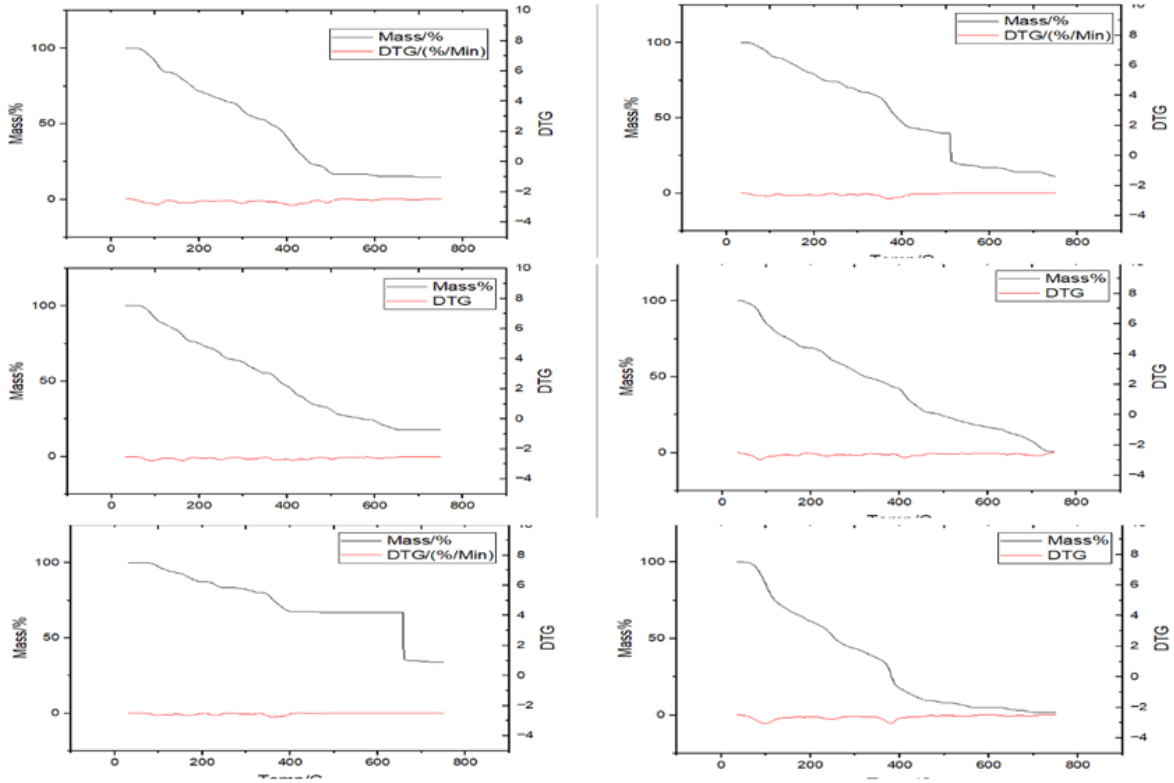

Figure 5:TGA and DTG Results of samples (1-6)

TGA AND DTG RESULTS

Thermal analysis demonstrates multiple stages of decomposition from 75 °C to 450 °C and validates that samples are thermally stable up to 450 °C. This corresponds to what [15] supposed. The initial decrease in weight at nearly 100 °C was ascribed to the dissolution of water (endothermic reaction). A second weight loss was noted at 200 ◦C, which can be attributed to adsorbed water within the cages, and a little weight loss was observed for the solvent that is physically adsorbed in internal pores [18]. The organic ligand BTC starts to burn out at about 338 °C (exothermic reaction).

Following the analysis, the mass remained, and assuming that this mostly relates to FeXOY. These results are fairly close and fall into the same temperature range when we compare them to the findings of the study carried out by Aguilar and colleagues [19]. This conclusion relates to the water responsible for the weight loss at almost 100 °C. Around 200 °C, a new weight loss step was noted; this can be attributed to adsorbed water in the cages. The organic ligand BTC start to burn out at about 318 °C, which resulted a multiple stages of decomposition, and all the samples are thermally stable up to 450 °C.

weight loss of the original sample. After the analysis, the mass was left, and it is probable that Fe2O3 makes up the majority of that mass.

UV-VIS DIFFUSE REFLECTANCE RESULTS5

Using a UV-visible spectrophotometer, diffuse reflectance spectroscopy (DRS) is a method commonly used to investigate the optical characteristics of solids.

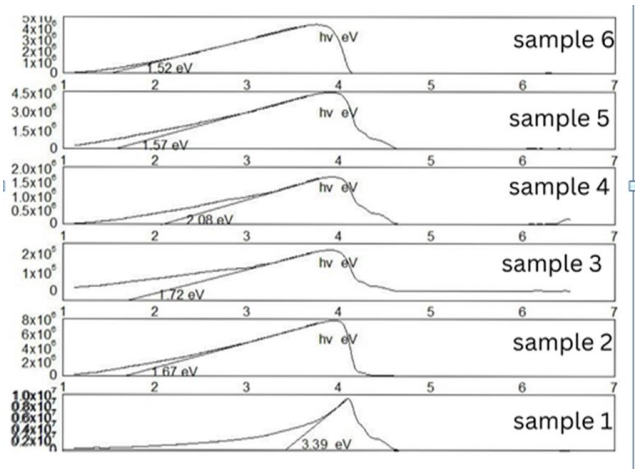

Figure 6: Band gap values of the samples (1-6)

Table 4: Band gap values of the samples (1-6)

Sample No	Band Gab (eV)
Sample 1	3.39
Sample 2	1.67
Sample 3	1.72
Sample 4	2.08
Sample 5	1.57
Sample 6	1.52

We can say that all samples, as shown in figure 6, with the exception of sample No. 1 (insulator), are semiconductors because materials with a band gap of less than three (Eg<3.0eV) are semiconductors, and those with a band gap of greater than three are insulators (Eg> 3.0eV) . [20]

CONCLUSION

There were six resulted samples, which varied in the proportions of the two elements with BTC. Over all, this work showed that all the samples have the same XRD pattern of MIL-100. The EDX results show that the substitution of iron by titanium happens in different proportions in each sample, and the SEM confirmed the results of the XRD calculations, which showed that most of the samples were nanoparticles.

The FT-IR results support the conclusions of the XRD results and show that the M-M bond formed in every sample, thermal analysis demonstrates

From UV-VIS, we conclude that sample No. 1 (insulators) has a band gap greater than three (Eg >3.0 eV), and all the others are semiconductors because their band gap is less than three (Eg < 3.0 eV).

REFERENCES:

1. Anja Cara,b*, Chrtomir Stropnika, Klaus-Viktor Peinemannb, Desalination 200 (2006) 424-426.

2. Ma, F. J., Liu, S. X., Sun, C. Y., Liang, D. D., Ren, G. J., Wei, F., ... & Su, Z. M. (2011). A sodalite-type porous metal− organic framework with polyoxometalate templates: adsorption and decomposition of dimethyl methyl phosphonate. Journal of the American Chemical Society, 133(12), 4178-4181.

3. Krungleviciute et al., 2007Ma, F. J., Liu, S. X., Sun, C. Y., Liang, D. D., Ren, G. J., Wei, F., ... & Su, Z. M. (2011). A sodalite-type porous metal− organic framework with polyoxometalate templates: adsorption and decomposition of dimethyl methylphosphonate. Journal of the American Chemical Society,133(12), 4178-4181.

4. Czaja, A. U., Trukhan, N., & Müller, U. (2009). Industrial applications of metal–organic frameworks. Chemical Society Reviews, 38(5), 1284-1293.

5. Tranchemontagne, D. J., Mendoza-Cortés, J. L., O'keeffe, M., & Yaghi, O. M. (2009). Secondary building units, nets and bonding in the chemistry of metal- organic frameworks. Chemical Society Reviews, 38(5), 1257-1283.

6. Sharmin, E., & Zafar, F. (2016). Introductory chapter: metal organic frameworks (MOFs). In Metal-organic frameworks. Intech Open.

7. Karmakar, A., & Oliver, C. L. (2013). A two-dimensional metal organic network with 1, 3, 5-benzenetricarboxylate and cobalt (II) ions: synthesis, structure and topology.

8. P. Horcajada, et al., "Synthesis and Catalytic properties of MIL-100(Fe), an iron (III) carboxylate with Large Pores", Chem. Commun., 2820-2822 (2007).

9. Castells-Gil, J., Padial, N. M., Almora-Barrios, N., Da Silva, I., Mateo, D., Albero, J., ... & Martí-Gastaldo, C. (2019). De novo synthesis of mesoporous photoactive titanium (iv)–organic frameworks with MIL-100 topology. Chemical Science, 10(15), 4313-4321.

10. Pangkumhang, B. H. U. C. K. C. H. A. N. Y. A., Jutaporn, P. A. N. I. T. A. N., Sorachoti, K., Khamdahsag, P., & Tanboonchuy, V. (2019). Applicability of iron (III) Trimesic (Fe-BTC) to enhance lignin separation from pulp and paper wastewater. Sains Malaysiana,48(1), 199-208

11. Jing Shi, Shengtao Hei, Huanhuan Liu, Yanghe Fu, Fumin Zhang, Yijun Zhong, Weidong Zhu 03 October 2013 https://doi.org/10.1155/2013/792827

12. Hakim, L., Dirgantara, M., and Nawir, M. (2019). Karakterisasi struktur material pasir bongkahan galian golongan c dengan menggunakan X-Ray Difraction (X-RD) di kota Palangkaraya. Jurnal Jejaring Matematika dan Sains, 1(1), 44-51.

13. Bunaciu, A. A., UdriŞTioiu, E. G., and Aboul-Enein, H. Y. (2015). X-ray diffraction: Instrumentation and applications. Critical Reviews in Analytical Chemistry, 45(4), 289-299.

14. Delgado-Marín, J. J., Narciso, J., & Ramos-Fernández, E. V. (2022). Effect of the Synthesis Conditions of MIL-100(Fe) on Its Catalytic Properties and Stability under Reaction Conditions. Materials (Basel, Switzerland),15(18), 6499. https://doi.org/10.3390/ma15186499

15. Lestari, W. W., Hartono, J., Adreane, M., Nugrahaningtyas, K. D., Purnawan, C., & Rahardjo, S. B. (2016). Electro-synthetic optimization of host material based on MIL-100 (Fe).Molekul, 11(1), 61-70.

16. Święch, Dominika & Paluszkiewicz, Czeslawa & Piergies, Natalia & Pięta, Ewa & Lelek-Borkowska, Urszula & Kwiatek, Wojciech. (2018). Identification of Corrosion Products on Fe and Cu Metals using Spectroscopic Methods. Acta Physica Polonica A. 133. 286-288. 10.12693/APhysPolA.133.286

17. Al-Amin, Mohammad & Dey, Shaikat & Rashid, Taslim & Ashaduzzaman, Md & Shamsuddin, Sayed. (2016). Solar Assisted Photocatalytic Degradation of Reactive Azo Dyes in Presence of Anatase Titanium Dioxide. 2. 14-21

18. Schlichte, K., Kratzke, T., & Kaskel, S. (2004). Improved synthesis, thermal stability and catalytic properties of the metal-organic framework compound Cu3(BTC)2 Microporous and Mesoporous Materials,73(1-2), 81-88.

19. Salazar-Aguilar, A. D., Vega, G., Casas, J. A., Vega-Díaz, S. M., Tristan, F., Meneses-Rodríguez, D., ... & Quintanilla, A. (2020). Direct hydroxylation of phenol to dihydroxy benzenes by H2O2 and fe-based metal-organic framework catalyst at room temperature. Catalysts, 10(2), 172.

20. Vu, H. T., Nguyen, M. B., Vu, T. M., Le, G. H., Pham, T. T., Nguyen, T. D., & Vu, T. A. (2020). Synthesis and application of novel nano Fe-BTC/GO composites as highly efficient photocatalysts in the dye degradation.Topics in Catalysis, 63, 1046- 1055.